Upscaled model for the diffusion/heterogeneous reaction in porous media: Boundary layer problem

Tien Dung Le, Christian Moyne, Mohamed Khaled Bourbatache, Olivier Millet

Upscaled model for the diffusion/heterogeneous reaction in porous media: boundary layer problem

Tien Dung Le[a,*], Christian Moyne[a], Mohamed Khaled Bourbatache[b], Olivier Millet[c]

[a] *University of Lorraine, CNRS, LEMTA, F-54000 Nancy, France*
[b] *Institut National des Sciences Appliquées, Laboratoire de Génie Civil et de Génie Mécanique, F-35000 Rennes, France*
[c] *Université de La Rochelle, CNRS, Laboratoire des Sciences de l'Ingénieur pour l'Environnement, F-17000 La Rochelle, France*

Abstract

Multi-species diffusion/heterogeneous reaction coupled problem in porous media involving a boundary layer problem is studied. The spectral approach developed in our previous work allows to derive a macroscopic model in the high Damköhler number regime combining homogenization technique and spectral approach. Such a homogenized model cannot describe the perturbation at the external boundary where the chemical equilibrium is not necessarily satisfied. We construct herein a modified model involving additional variables, which are rapidly-decaying functions, to capture the complex physics in the boundary layer. Numerical simulations underline the accuracy of the proposed correction in both steady and transient states.

Keywords: Homogenization, Diffusion/reaction problem, Spectral approach, Boundary layer problem

1. Introduction

Reactive transport of multi-species in porous media, which is of major interest for many applications in numerous areas such as electrochemical systems, agronomy, geology, etc., has received considerable attention from the modeling point of view. Macroscopic models involving effective coefficients can be rigorously derived from upscaling approaches [1, 2, 3, 4, 5, 6, 7, 8, 9]. A challenging case refers to the predominant reaction situation when the medium exhibits a complex behavior

*Corresponding author
Email addresses: tien-dung.le@univ-lorraine.fr (Tien Dung Le), christian.moyne@univ-lorraine.fr (Christian Moyne), mohamed-khaled.bourbatache@insa-rennes.fr (Mohamed Khaled Bourbatache), olivier.millet@univ-lr.fr (Olivier Millet)

and the effective coefficients in the macroscopic equations depend on reaction rates [1, 3, 10]. More sophisticated models are required to accurately describe the non-equilibrium state at very short times that are of the order of the characteristic reaction time [11, 12]. In spite of the difficulty, macroscopic models were derived by using the periodic homogenization technique and a spectral approach in our previous work [13, 14, 15]. However, the homogenization procedure imposes a spatial periodicity condition at the boundary of the unit cell. In this framework, the physics inside the porous domain can be accurately captured by the macroscopic models while at the outer surface of the domain, periodicity conditions cannot be respected. This leads to a boundary layer problem depending on the boundary condition type.

The boundary layer problems have been widely studied for elastic periodic composites [16, 17], for elastic beams [18], for elastic shells [19] or in a more general way in [20, 21]. Matine et al. [22, 23] proposed to extend this approach for thermal problem in periodic structures, to take into account the edge effects. However, to the best of our knowledge there is practically no work in the literature addressing the boundary layer problem for the coupling of predominating reaction and diffusion of multi-species in porous media.

In a sequence of papers, the coupling of diffusion/reaction of two species with different molecular diffusion coefficients has been studied combining periodic homogenization technique with a spectral approach [13, 14, 15, 24]. Concentrations of the initial pore-scale problem are expanded into a series development related to a spectral problem defined in a unit cell, yielding a new local problem to be homogenized. This approach is able to capture the complex coupling at short times when the chemical equilibrium is not reached. However, such a macroscopic model cannot provide information about the boundary layer that develops in the vicinity of the outer boundary due to the boundary conditions. In this work, corrections are added to the macroscopic model to take into account the boundary conditions at the outer boundary of the domain. In steady state, terms of the first order need to be corrected by introducing new variables whereas in transient regime, corrections at lower order are added to capture the perturbation in the boundary layer at short times. Such a modification implies new closure variables that must be solved over several unit cells from the edge of the domain. For larger distances, these decreasing functions vanish.

The paper is organized as follows. In Section 2, the main result of the upscaling procedure based on the spectral approach and homogenization technique for high Damköhler number is recalled. Section 3 is devoted to the development of the modified model in order to address the boundary layer

problem in both steady and transient regimes. Numerical simulations are performed in Section 4 to validate the proposed model and to underline the importance of the correction terms. Conclusions are drawn in Section 5.

2. Macroscopic model for high Damköhler number: a recall

In this section, the main steps and results of the homogenization procedure to derive the macroscopic equations for the diffusion-reaction problem, developed in a previous work [14] are recalled. To simplify the notation, the superscript * indicating dimensional quantities in the preceding reference is omitted.

A porous medium occupying a macroscopic domain Ω with a characteristic length L, is composed of an immobile fluid phase Ω_f and of a rigid solid phase Ω_s with a solid-fluid interface Γ_{fs}. The medium is constituted of the repetition of a periodic elementary cell $Y = Y_f \cup Y_s$ of characteristic length l, composed of the fluid phase Y_f and the solid phase Y_s together with the solid-fluid interface ∂Y_{fs}. The boundary $\partial Y = \partial Y_{fs} \cup \partial Y_e$ is constituted of the fluid-solid interface ∂Y_{fs} assumed to be impervious and of the external interface $\partial Y_e = \partial Y_{se} \cup \partial Y_{fe}$ separating two juxtaposed elementary cells. The macroscopic and microscopic spatial coordinates are $\mathbf{x} = (x_1, x_2, x_3)$ and $\mathbf{y} = (y_1, y_2, y_3)$ respectively. The scale separation ($l \ll L$) allows the introduction of the small parameter $\varepsilon = l/L$.

Let c_1 and c_2 be the concentrations of species A and B respectively. The transport is ruled by a Fickian process. On the fluid-solid interface Γ_{fs}, linear chemical reactions exchange species A and B. The microscopic diffusion/reaction equations at the pore-scale are written as

$$\left\{\begin{array}{rcll} \dfrac{\partial c_1}{\partial t} - \boldsymbol{\nabla}\cdot(\mathcal{D}_1\boldsymbol{\nabla}c_1) &=& 0 & \text{in } \Omega_f \\ \dfrac{\partial c_2}{\partial t} - \boldsymbol{\nabla}\cdot(\mathcal{D}_2\boldsymbol{\nabla}c_2) &=& 0 & \text{in } \Omega_f \\ -\mathcal{D}_1\boldsymbol{\nabla}c_1\cdot\mathbf{n}_{fs} &=& k_1c_1 - k_2c_2 & \text{at } \Gamma_{fs} \\ -\mathcal{D}_2\boldsymbol{\nabla}c_2\cdot\mathbf{n}_{fs} &=& k_2c_2 - k_1c_1 & \text{at } \Gamma_{fs} \end{array}\right. \tag{1}$$

where $\mathcal{D}_1$ and $\mathcal{D}_2$ denote the diffusion coefficients of A and B respectively, k_1 and k_2 the reaction rates. These coefficients have constant values during the process. $\mathbf{n}_{fs}$ is the normal unit vector at the solid/fluid interface pointing out of the fluid phase. The microscopic problem is completed by the initial conditions for given values of $c_1(t=0)$ and $c_2(t=0)$ and the boundary conditions at the outer edges of the domain. In this work, we only consider the Dirichlet conditions in which the concentrations are given at the edges.

The initial model is transformed into a new problem associated with the following periodic spectral problem defined on the periodic unit cell Y

$$\left\{\begin{array}{rcll} -\boldsymbol{\nabla}\cdot(\mathcal{D}_1\boldsymbol{\nabla}\psi_{1,n}) &=& \lambda_n\psi_{1,n} & \text{in } Y_f \\ -\boldsymbol{\nabla}\cdot(\mathcal{D}_2\boldsymbol{\nabla}\psi_{2,n}) &=& \lambda_n\psi_{2,n} & \text{in } Y_f \\ -\mathcal{D}_1\boldsymbol{\nabla}\psi_{1,n}\cdot\mathbf{n}_{fs} &=& k_1\,\psi_{1,n} - k_2\,\psi_{2,n} & \text{at } \partial Y_{fs} \\ -\mathcal{D}_2\boldsymbol{\nabla}\psi_{2,n}\cdot\mathbf{n}_{fs} &=& k_2\,\psi_{2,n} - k_1\,\psi_{1,n} & \text{at } \partial Y_{fs} \end{array}\right. \tag{2}$$

where $\psi_{1,n}(\mathbf{y})$ and $\psi_{2,n}(\mathbf{y})$ represent the succesive eigenfunctions sharing the same positive eigenvalue λ_n ordered in ascending order with $n \in \mathbb{N}$. The eigenfunctions $\psi_{1,n}(\mathbf{y})$ and $\psi_{2,n}(\mathbf{y})$ are defined within a same multiplicative constant, which can be determined according to

$$k_1 \left\langle \psi_{1,n}^2 \right\rangle^f + k_2 \left\langle \psi_{2,n}^2 \right\rangle^f = k_1 + k_2 \tag{3}$$

where $\langle\ \rangle^f$ denotes the volume average over the fluid phase.

For $n = 0$, $\lambda_0 = 0$ and the two eigenfunctions are constant satisfying the condition $k_1\psi_{1,0} - k_2\psi_{2,0} = 0$. They are given by

$$\psi_{1,0} = \sqrt{\frac{k_2}{k_1}}, \qquad \psi_{2,0} = \sqrt{\frac{k_1}{k_2}} \tag{4}$$

Finally note that for $n \geq 1$

$$\langle \psi_{1,n} \rangle^f + \langle \psi_{2,n} \rangle^f = 0 \tag{5}$$

resulting from the compatibility condition of Eqs. (2).

c_i ($i \in \{1,2\}$) are then sought in an expansion related to the spectral problem (2) as follows

$$c_i(t,\mathbf{x},\mathbf{y}) = \sum_{n=0}^{\infty} \psi_{i,n}(\mathbf{y})\ \exp\left(-\lambda_n t\right)\ v_{i,n}(t,\mathbf{x},\mathbf{y}) \tag{6}$$

with new variables $v_{i,n}$ depending on time and position.

Let define the macroscopic Damköhler number Da_L as the ratio of the macroscopic diffusion time to the reaction one

$$\mathrm{Da}_L = \frac{k_r L}{\mathcal{D}_r} \tag{7}$$

where k_r and $\mathcal{D}_r$ denote reference reaction rate and diffusion coefficient. In [14], the Damköhler number appears naturally through the dimensional analysis which has been skipped in this summary

of the results. The reference time is chosen as the macroscopic diffusion time $t_r = L^2/\mathcal{D}_r$. The reader can refer to [14] for more details on the procedure.

It has been shown in [14] that for small Damköhler number of order $\mathcal{O}(\varepsilon)$, a classical homogenization procedure can correctly predict the macroscopic laws. However, for higher Damköhler number of order $\mathcal{O}(\varepsilon^0)$ or $\mathcal{O}(\varepsilon^{-1})$, special development is needed to precisely predict the behavior of diffusion/reaction mechanism for short time [14]. It should be noted that a slight difference between the two cases $\mathcal{O}(\varepsilon^0)$ and $\mathcal{O}(\varepsilon^{-1})$ comes from the closure problem in solid/fluid interface condition. In this work, we deal with the most interesting case of high Damköhler number with $\mathrm{Da}_L = \mathcal{O}(\varepsilon^{-1})$. By inserting (6) in the initial problem (1) and making use of the definition (7), performing a dimensional analysis, the ε-microscopic model for $v_{i,n}$ in dimensional space reads as

$$\left\{\begin{array}{rcll} \psi_{1,n}^2 \dfrac{\partial v_{1,n}^{(\varepsilon)}}{\partial t} & = & \boldsymbol{\nabla}\cdot\left(\widetilde{\mathcal{D}}_{1,n}\boldsymbol{\nabla} v_{1,n}^{(\varepsilon)}\right) & \text{in } Y_f \\ \psi_{2,n}^2 \dfrac{\partial v_{2,n}^{(\varepsilon)}}{\partial t} & = & \boldsymbol{\nabla}\cdot\left(\widetilde{\mathcal{D}}_{2,n}\boldsymbol{\nabla} v_{2,n}^{(\varepsilon)}\right) & \\ -\widetilde{\mathcal{D}}_{1,n}\boldsymbol{\nabla} v_{1,n}^{(\varepsilon)}\cdot\mathbf{n}_{fs} & = & \varepsilon^{-1}k_2\,\psi_{1,n}\,\psi_{2,n}(v_{1,n}^{(\varepsilon)} - v_{2,n}^{(\varepsilon)}) & \text{at } \partial Y_{fs} \\ -\widetilde{\mathcal{D}}_{2,n}\boldsymbol{\nabla} v_{2,n}^{(\varepsilon)}\cdot\mathbf{n}_{fs} & = & \varepsilon^{-1}k_1\,\psi_{1,n}\,\psi_{2,n}(v_{2,n}^{(\varepsilon)} - v_{1,n}^{(\varepsilon)}) & \end{array}\right. \tag{8}$$

with $\widetilde{\mathcal{D}}_{1,n} = \mathcal{D}_1\psi_{1,n}^2$ and $\widetilde{\mathcal{D}}_{2,n} = \mathcal{D}_2\psi_{2,n}^2$. By collecting the terms in the different powers of ε, one leads to the following results.

• **Slow variables:** At the leading order, the solution of v is $v_{1,n}^{(0)}(t,\mathbf{x},\mathbf{y}) = v_{2,n}^{(0)}(t,\mathbf{x},\mathbf{y}) = v_n^{(0)}(t,\mathbf{x})$.

• **Fluctuation:** the solution for $v_{1,n}^{(1)}$ and $v_{2,n}^{(1)}$ are sought in the following form, to within one additive constant $\widehat{v}_n^{(1)}$ depending on t and $\mathbf{x}$[1]

$$\begin{array}{rcl} v_{1,n}^{(1)} & = & \boldsymbol{\chi}_{1,n}(\mathbf{y})\cdot\boldsymbol{\nabla}_x v_n^{(0)}(t,\mathbf{x}) + \widehat{v}_n^{(1)}(t,\mathbf{x}) \\ v_{2,n}^{(1)} & = & \boldsymbol{\chi}_{2,n}(\mathbf{y})\cdot\boldsymbol{\nabla}_x v_n^{(0)}(t,\mathbf{x}) + \widehat{v}_n^{(1)}(t,\mathbf{x}) \end{array} \tag{9}$$

[1] This necessary condition comes from the right hand side of the associated boundary conditions in Eqs. (8)

where the vectors $\boldsymbol{\chi}_{1,n}$ and $\boldsymbol{\chi}_{2,n}$ satisfy the closure problem[2]

$$\left\{\begin{array}{rcll} 0 & = & \boldsymbol{\nabla}_y \cdot \left[\widetilde{\mathcal{D}}_{1,n}\left(\boldsymbol{I}+\boldsymbol{\nabla}_y\boldsymbol{\chi}_{1,n}\right)\right] & \text{in } Y_f \\ 0 & = & \boldsymbol{\nabla}_y \cdot \left[\widetilde{\mathcal{D}}_{2,n}\left(\boldsymbol{I}+\boldsymbol{\nabla}_y\boldsymbol{\chi}_{2,n}\right)\right] & \\ -\widetilde{\mathcal{D}}_{1,n}\mathbf{n}_{fs}\cdot\left(\boldsymbol{I}+\boldsymbol{\nabla}_y\boldsymbol{\chi}_{1,n}\right) & = & k_2\psi_{1,n}\psi_{2,n}\left(\boldsymbol{\chi}_{1,n}-\boldsymbol{\chi}_{2,n}\right) & \text{at } \partial Y_{fs} \\ -\widetilde{\mathcal{D}}_{2,n}\mathbf{n}_{fs}\cdot\left(\boldsymbol{I}+\boldsymbol{\nabla}_y\boldsymbol{\chi}_{2,n}\right) & = & k_1\psi_{1,n}\psi_{2,n}\left(\boldsymbol{\chi}_{2,n}-\boldsymbol{\chi}_{1,n}\right) & \end{array}\right. \tag{10}$$

The particular case $n=0$ corresponds to the eigenvalue $\lambda_0=0$ and to the eigenfunctions (4). In this case $\boldsymbol{\chi}_{1,0}\equiv\boldsymbol{\chi}_{2,0}\equiv\boldsymbol{\chi}$ and the local problem (10) reduces to the standard closure problem

$$\left\{\begin{array}{rcll} \boldsymbol{\nabla}^2_{yy}\boldsymbol{\chi} & = & 0 & \text{in } Y_f \\ \left(\boldsymbol{I}+\boldsymbol{\nabla}_y\boldsymbol{\chi}\right)\cdot\mathbf{n}_{fs} & = & 0 & \text{at } \partial Y_{fs} \end{array}\right. \tag{11}$$

This leads to

$$v^{(1)}_{1,0}=v^{(1)}_{2,0}=v^{(1)}_0=\boldsymbol{\chi}(\mathbf{y})\cdot\boldsymbol{\nabla}_x v^{(0)}_0(t,\mathbf{x})+\hat{v}^{(1)}_0(t,\mathbf{x}) \tag{12}$$

- **Macroscopic equation:** the macroscopic problem for $v^{(0)}_n$ is derived as

$$\frac{\partial v^{(0)}_n}{\partial t} = \boldsymbol{\nabla}_x\cdot\left(\mathbf{D}_{v,n}\cdot\boldsymbol{\nabla}_x v^{(0)}_n\right) \tag{13}$$

where the effective diffusion tensor $\mathbf{D}_{v,n}$ is defined by

$$\mathbf{D}_{v,n}=\frac{k_1}{k_1+k_2}\left\langle\widetilde{\mathcal{D}}_{1,n}\left(\boldsymbol{I}+\left(\boldsymbol{\nabla}_y\boldsymbol{\chi}_{1,n}\right)^{\mathsf{T}}\right)\right\rangle^f+\frac{k_2}{k_1+k_2}\left\langle\widetilde{\mathcal{D}}_{2,n}\left(\boldsymbol{I}+\left(\boldsymbol{\nabla}_y\boldsymbol{\chi}_{2,n}\right)^{\mathsf{T}}\right)\right\rangle^f \tag{14}$$

For $n=0$, the effective tensor is given by

$$\mathbf{D}_{v,0}=\frac{k_1\mathcal{D}_2+k_2\mathcal{D}_1}{k_1+k_2}\langle\boldsymbol{I}+\left(\boldsymbol{\nabla}_y\boldsymbol{\chi}\right)^{\mathsf{T}}\rangle^f \tag{15}$$

- **Macroscopic equations for the concentrations:** As discussed in [14], only the two first eigenvalues $\lambda_0=0$ and λ_1 with their corresponding eigenfunctions are considered. In the asymptotic

[2] Here, rather than using the tensorial definition in [14] in which a transpose operator is needed, the index notation for the gradient of a vector defined in [25] is adopted.

development (6), the higher order terms can be ignored due to the exponential decay in time. The averaged concentrations at the leading order are given by

$$\begin{aligned}\langle c_1^{(0)}\rangle^f &= \psi_{1,0}\; v_0^{(0)} + \langle \psi_{1,1}\rangle^f \exp(-\lambda_1 t)\; v_1^{(0)}\\ \langle c_2^{(0)}\rangle^f &= \psi_{2,0}\; v_0^{(0)} + \langle \psi_{2,1}\rangle^f \exp(-\lambda_1 t)\; v_1^{(0)}\end{aligned} \tag{16}$$

Omitting for the sake of simplicity the subscript (0) related to the scale order, using (13) for $n = 0$ and $n = 1$, and considering the time derivative of (16) and the compatibility condition (5) for $n = 1$ result in the following mass conservation equations at the leading order[3]:

$$\left\{\begin{array}{ll} \dfrac{\partial\langle c_1\rangle^f}{\partial t} & -\boldsymbol{\nabla}_x\cdot\left(\dfrac{k_1\mathbf{D}_{v,1}+k_2\mathbf{D}_{v,0}}{k_1+k_2}\cdot\boldsymbol{\nabla}_x\langle c_1\rangle^f\right)\\ & -\boldsymbol{\nabla}_x\cdot\left(\dfrac{k_2(\mathbf{D}_{v,0}-\mathbf{D}_{v,1})}{k_1+k_2}\cdot\boldsymbol{\nabla}_x\langle c_2\rangle^f\right)+\lambda_1\dfrac{k_1\langle c_1\rangle^f-k_2\langle c_2\rangle^f}{k_1+k_2}=0\\ \dfrac{\partial\langle c_2\rangle^f}{\partial t} & -\boldsymbol{\nabla}_x\cdot\left(\dfrac{k_1(\mathbf{D}_{v,0}-\mathbf{D}_{v,1})}{k_1+k_2}\cdot\boldsymbol{\nabla}_x\langle c_1\rangle^f\right)\\ & -\boldsymbol{\nabla}_x\cdot\left(\dfrac{k_2\mathbf{D}_{v,1}+k_1\mathbf{D}_{v,0}}{k_1+k_2}\cdot\boldsymbol{\nabla}_x\langle c_2\rangle^f\right)-\lambda_1\dfrac{k_1\langle c_1\rangle^f-k_2\langle c_2\rangle^f}{k_1+k_2}=0\end{array}\right. \tag{17}$$

Given the effective coefficient tensors $\mathbf{D}_{v,0}$ and $\mathbf{D}_{v,1}$, and the initial and boundary conditions, the coupled diffusion-reaction Eqs. (17) can be solved to compute the concentration profiles.

3. Boundary layer problem

The macroscopic model based on the homogenization technique relies on the periodic condition hypothesis. As a consequence, it cannot capture the boundary layer problem developed in the vicinity of the edge of the domain when an outer boundary condition of Dirichlet type is imposed. In this section, corrections are made to precisely take into account this boundary layer in the upscaled problem.

Let consider a parallelepiped rectangular porous medium with macro and microscopic coordinates $\{x_1, x_2, x_3\}$ and $\{y_1, y_2, y_3\}$ respectively[4]. At the inlet boundary $x_1 = 0$ (and $y_1 = 0$),

[3] Eqs. (17) are dimensional equations corresponding to Eqs. (49) of [14], where the stars have been omitted.

[4] It should be noted that the semi-infinite domain $x_1 \in [0, \infty]$, $x_2, x_3 \in [-\infty, \infty]$ can be reduced to a parallelepiped when the periodic conditions in x_2 and x_3 directions are applied and a finite region in the vicinity of the boundary is considered for the boundary layer problem

Dirichlet conditions for the concentrations, $c_1 = c_{1D}$ and $c_2 = c_{2D}$ are imposed. The most interesting case is when $k_1 c_{1D} \neq k_2 c_{2D}$ corresponding to a non-equilibrium situation. This leads to a thin boundary layer for the concentration profiles in the vicinity of the interface $x_1 = 0$. Our main objective is to incorporate this layer in the upscaled model. To accomplish this task, we first consider the development (6) with the two first orders in ε and the two first eigenvalues together with the corresponding eigenfunctions:

$$\begin{aligned} c_1 &= \sqrt{\frac{k_2}{k_1}}\left(v_0^{(0)} + v_0^{(1)}\right) + \psi_{1,1}(\mathbf{y})\exp(-\lambda_1 t)\left(v_1^{(0)} + v_{1,1}^{(1)}\right) \\ c_2 &= \sqrt{\frac{k_1}{k_2}}\left(v_0^{(0)} + v_0^{(1)}\right) + \psi_{2,1}(\mathbf{y})\exp(-\lambda_1 t)\left(v_1^{(0)} + v_{2,1}^{(1)}\right) \end{aligned} \tag{18}$$

It should be noted that the formal parameter ε can be omitted for the calculation of the concentrations. This is a quasi-exact solution in the domain, except for the boundary layer in the vicinity of the interface where boundary conditions should be imposed for the variable $v_0^{(0)}$ in order to solve the problem (13). Two distinct problems related to the permanent and transient regimes need to be considered.

3.1. Steady state

In the steady state when $t \to \infty$, only the first order variable $v_0^{(0)}$ and second order variable $v_0^{(1)}$, both related to the zero eigenvalue, play a role in the boundary layer. To take into account the boundary layer, the expansion of the concentrations needs to be improved in the sense of [20]. Considering Dirichlet conditions, since two boundary values c_{1D} and c_{2D} are given for the concentrations and only one variable $v_0^{(0)}$ is involved at the interface, it is necessary to introduce new boundary variables $u_{1BL}^{(0)}(\mathbf{x},\mathbf{y})$ and $u_{2BL}^{(0)}(\mathbf{x},\mathbf{y})$ at order $\mathcal{O}\left(\varepsilon^0\right)$ and $v_{0,BL}^{(1)}$ at order $\mathcal{O}\left(\varepsilon^1\right)$ as

$$\begin{aligned} c_1 &= \sqrt{\frac{k_2}{k_1}}\left(v_0^{(0)} + v_0^{(1)} + v_{0,BL}^{(1)}\right) + u_{1BL}^{(0)} \\ c_2 &= \sqrt{\frac{k_1}{k_2}}\left(v_0^{(0)} + v_0^{(1)} + v_{0,BL}^{(1)}\right) + u_{2BL}^{(0)} \end{aligned} \tag{19}$$

It should be underlined that the boundary layer problem needs to be solved in a reduced fluid domain $Y_f^\dagger$ (with a corresponding solid/fluid interface $\partial Y_{fs}^\dagger$) composed of the infinite repetition of the unit cell Y in the direction Oy_1 perpendicular to the edge.

3.1.1. Order $\mathcal{O}(\varepsilon^0)$

Inserting (19) in the initial problem (1) in steady state, the problem for $u_{1BL}^{(0)}$ and $u_{2BL}^{(0)}$ in the boundary layer at order $\mathcal{O}(\varepsilon^{-2})$ in volume and $\mathcal{O}(\varepsilon^{-1})$ at the interface reads as

$$\left\{\begin{array}{rcll} 0 & = & \boldsymbol{\nabla}_y \cdot \left(\mathcal{D}_1 \boldsymbol{\nabla}_y u_{1BL}^{(0)}\right) & \text{in } Y_f^\dagger \\ 0 & = & \boldsymbol{\nabla}_y \cdot \left(\mathcal{D}_2 \boldsymbol{\nabla}_y u_{2BL}^{(0)}\right) & \\ -\mathcal{D}_1 \boldsymbol{\nabla}_y u_{1BL}^{(0)} \cdot \mathbf{n}_{fs} & = & k_1 u_{1BL}^{(0)} - k_2 u_{2BL}^{(0)} & \text{on } \partial Y_{fs}^\dagger \\ -\mathcal{D}_2 \boldsymbol{\nabla}_y u_{2BL}^{(0)} \cdot \mathbf{n}_{fs} & = & k_2 u_{2BL}^{(0)} - k_1 u_{1BL}^{(0)} & \end{array}\right. \tag{20}$$

$u_{1BL}^{(0)}$ and $u_{2BL}^{(0)}$ are periodic in y_2 and y_3 and satisfy the following boundary conditions

$$\begin{array}{lll} y_1 = 0 & c_{1D} = \sqrt{\dfrac{k_2}{k_1}} v_{0D}^{(0)} + u_{1BL}^{(0)}(y_1 = 0) & \\ & c_{2D} = \sqrt{\dfrac{k_1}{k_2}} v_{0D}^{(0)} + u_{2BL}^{(0)}(y_1 = 0) & \\ y_1 \to \infty & u_{1BL}^{(0)}(y_1) \to 0 & \\ & u_{2BL}^{(0)}(y_1) \to 0 & \end{array} \tag{21}$$

where $v_{0D}^{(0)}$ is the unknown Dirichlet condition value of $v_0^{(0)}$ at $y_1 = 0$. The problem (20) can be transformed by introducing the auxiliary variables

$$\begin{array}{rcl} s_{BL}^{(0)} & = & \mathcal{D}_1 u_{1BL}^{(0)} + \mathcal{D}_2 u_{2BL}^{(0)} \\ d_{BL}^{(0)} & = & k_1 u_{1BL}^{(0)} - k_2 u_{2BL}^{(0)} \end{array} \tag{22}$$

Inserting the above definitions in (20), the problems for $s_{BL}^{(0)}$ and $d_{BL}^{(0)}$ are separate and given by

$$\left\{\begin{array}{rcll} 0 & = & \Delta_{yy} s_{BL}^{(0)} & \text{in } Y_f^\dagger \\ 0 & = & \Delta_{yy} d_{BL}^{(0)} & \\ -\boldsymbol{\nabla}_y s_{BL}^{(0)} \cdot \mathbf{n}_{fs} & = & 0 & \text{on } \partial Y_{fs}^\dagger \\ -\boldsymbol{\nabla}_y d_{BL}^{(0)} \cdot \mathbf{n}_{fs} & = & \left(\dfrac{k_1}{\mathcal{D}_1} + \dfrac{k_2}{\mathcal{D}_2}\right) d_{BL}^{(0)} & \end{array}\right. \tag{23}$$

$s_{BL}^{(0)}$ and $d_{BL}^{(0)}$ are also periodic in y_2 and y_3. In addition, by using the definitions (22) of $s_{BL}^{(0)}$ and $d_{BL}^{(0)}$ in (21), one obtains the following boundary conditions

$$\begin{array}{lll} y_1 = 0 & s_{BL}^{(0)} = \mathcal{D}_1 c_{1D} + \mathcal{D}_2 c_{2D} - \dfrac{k_1 \mathcal{D}_2 + k_2 \mathcal{D}_1}{\sqrt{k_1 k_2}} v_{0D}^{(0)} & \\ & d_{BL}^{(0)} = d_D = k_1 c_{1D} - k_2 c_{2D} & \\ y_1 \to \infty & s_{BL}^{(0)}(y_1) \to 0 & \\ & d_{BL}^{(0)}(y_1) \to 0 & \end{array} \tag{24}$$

In steady state, the solution of the problem (23) for $s_{BL}^{(0)}$ is a constant equal to 0 due to the boundary condition (24) at $y_1 \to \infty$. From (24), the Dirichlet condition for $v_0^{(0)}$ at $y_1 = 0$ reads as

$$v_{0D}^{(0)} = \sqrt{k_1 k_2}\frac{\mathcal{D}_1 c_{1D} + \mathcal{D}_2 c_{2D}}{k_1\mathcal{D}_2 + k_2\mathcal{D}_1} \tag{25}$$

so that at the leading order, the boundary values of the concentrations imposed at $x_1 = 0$ to calculate the solution of the inner problem (17) are given by

$$\left\{\begin{array}{rcccl} c_{1D}^{(0)} & = & \sqrt{\dfrac{k_2}{k_1}}v_{0D}^{(0)} & = & k_2\dfrac{\mathcal{D}_1 c_{1D} + \mathcal{D}_2 c_{2D}}{k_1\mathcal{D}_2 + k_2\mathcal{D}_1} \\ c_{2D}^{(0)} & = & \sqrt{\dfrac{k_1}{k_2}}v_{0D}^{(0)} & = & k_1\dfrac{\mathcal{D}_1 c_{1D} + \mathcal{D}_2 c_{2D}}{k_1\mathcal{D}_2 + k_2\mathcal{D}_1} \end{array}\right. \tag{26}$$

Inserting (25) into (21) gives the boundary values for $u_{1BL}^{(0)}$ and $u_{2BL}^{(0)}$

$$\left\{\begin{array}{rcl} u_{1BL(}^{(0)}(y_1 = 0) & = & \mathcal{D}_2\dfrac{k_1 c_{1D} - k_2 c_{2D}}{k_1\mathcal{D}_2 + k_2\mathcal{D}_1} \\ u_{2BL(}^{(0)}(y_1 = 0) & = & \mathcal{D}_1\dfrac{k_2 c_{2D} - k_1 c_{1D}}{k_1\mathcal{D}_2 + k_2\mathcal{D}_1} \end{array}\right. \tag{27}$$

It should be noted that the problem for $d_{BL}^{(0)}$ in (23) and (24) is an exponential decay problem-type involving a thin boundary layer affected by this correction.

To summarize, in steady state, at the order $\mathcal{O}(\varepsilon^0)$, to capture the boundary layer problem when the Dirichlet conditions for the concentrations do not verify the equilibrium condition, the problems for $v_0^{(0)}$ (Eq. (13) for $n = 0$) and for $u_{1BL}^{(0)}$ and $u_{2BL}^{(0)}$ (Eq. (20)) must be solved with the boundary values for $v_0^{(0)}$, $u_{1BL}^{(0)}$ and $u_{2BL}^{(0)}$ given by (25) and (27) respectively. The concentrations c_1 and c_2 must be adjusted by a thin boundary layer involving $u_{1BL}^{(0)}$ and $u_{2BL}^{(0)}$.

3.1.2. Order $\mathcal{O}(\varepsilon^1)$

This correction comes from the fact that in the concentrations given by (18), the term $v_0^{(1)}$ is not uniform in space at the boundary $y_1 = 0$. Similarly to the expression (12) for $v_0^{(1)}$, the boundary correction $v_{0,\mathrm{BL}}^{(1)}$ is sought in the form

$$v_{0,\mathrm{BL}}^{(1)} = \boldsymbol{\omega}\cdot\boldsymbol{\nabla}_x v_0^{(0)} \tag{28}$$

The vector $\boldsymbol{\omega}$ periodic in y_2 and y_3 must satisfy the closure

$$\left\{\begin{array}{rcll} \boldsymbol{\nabla}_{yy}^2\boldsymbol{\omega} & = & 0 & \text{in } Y_f^\dagger \\ -\boldsymbol{\nabla}_y\boldsymbol{\omega}\cdot\mathbf{n} & = & 0 & \text{on } \partial Y_{fs}^\dagger \end{array}\right. \tag{29}$$

At the boundary $y_1 = 0$ in order to satisfy the boundary condition $v_0^{(1)} + v_{0,BL}^{(1)} = 0$, we impose

$$\boldsymbol{\omega} + \boldsymbol{\chi} = 0 \tag{30}$$

where $\boldsymbol{\chi}$ is the solution of the closure problem (11). In the direction y_1 of unit vector $\mathbf{e}_1$, for $y_1 \to \infty$, a homogeneous Neuman condition is imposed

$$\boldsymbol{\nabla}_y \boldsymbol{\omega} \cdot \mathbf{e}_1 = 0 \tag{31}$$

The vector $\boldsymbol{\omega}$ will reach a constant value at large value of y_1 resulting from the averaging of the $\boldsymbol{\omega} = -\boldsymbol{\chi}$ values at the interface $y_1 = 0$. As this constant value must be 0, the indetermination of the $\boldsymbol{\chi}$ problem (11) is exploited subtracting this value from $\boldsymbol{\omega}$ [5].

In the particular case of a symmetrical unit cell, in the frame of the symmetry axes centered on the cell, imposing a null volume average ensures the unicity of $\boldsymbol{\chi}$ where the components χ_i are odd relative to y_i (and even relative to the other coordinates $y_{j\neq i}$). Therefore, if the external surface of the medium coincides with the surface of the unit cell Y of normal $\mathbf{e}_1$, χ_1 is null due to the combination of oddness and periodicity. Consequently, $\omega_1 = 0$ on the surface $y_1 = 0$ of $Y^\dagger$. Hence ω_1 is identically null in $Y_f^\dagger$. In conclusion, if the gradient $\boldsymbol{\nabla}_x v_0^{(0)}$ is parallel to $\mathbf{e}_1$, the correction $v_{0,\mathrm{BL}}^{(1)}$ is null over $Y_f^\dagger$.

3.2. Transient state

In the transient regime, the terms at order $\mathcal{O}(\varepsilon)$ in (18) must be corrected to better describe the complex unsteady non-equilibrium effect in the boundary layer. It is important to note that due to the large Damköhler number, the physical coupling is affected by the boundary condition only for short times. Beyond this time, the steady state is established. The $\mathcal{O}(\varepsilon^0)$-corrective terms for the two concentrations $u_{1,BL}^{(0)}$ and $u_{2,BL}^{(0)}$ are now transient. We also introduce the $\mathcal{O}(\varepsilon)$-corrective terms $v_{1,1\mathrm{BL}}^{(1)}$ and $v_{2,1\mathrm{BL}}^{(1)}$ into the expression of the concentrations (18) as

$$\begin{aligned} c_1 &= \sqrt{\frac{k_2}{k_1}}\left(v_0^{(0)} + v_0^{(1)} + v_{0,\mathrm{BL}}^{(1)}\right) + u_{1BL}^{(0)} + \psi_{1,1}(\mathbf{y})\exp(-\lambda_1 t)\left(v_1^{(0)} + v_{1,1}^{(1)} + v_{1,1\mathrm{BL}}^{(1)}\right) \\ c_2 &= \sqrt{\frac{k_1}{k_2}}\left(v_0^{(0)} + v_0^{(1)} + v_{0,\mathrm{BL}}^{(1)}\right) + u_{2BL}^{(0)} + \psi_{2,1}(\mathbf{y})\exp(-\lambda_1 t)\left(v_1^{(0)} + v_{2,1}^{(1)} + v_{2,1\mathrm{BL}}^{(1)}\right) \end{aligned} \tag{32}$$

[5] We recall that the boundary conditions are imposed for c_1 and c_2 at the main order, that implies according to (19) that $v_0^{(1)} + v_{0,BL}^{(1)} = 0$ at order $\mathcal{O}(\varepsilon)$.

3.2.1. Order $\mathcal{O}(\varepsilon^0)$

Let define the characteristic short time τ related to the macroscopic time t by $\tau = \varepsilon^{-2}t$. The transient problem for $u_{1BL}^{(0)}$ and $u_{2BL}^{(0)}$ depending on $\mathbf{y}$ then reads as

$$\left\{\begin{array}{rcll} \dfrac{\partial u_{1BL}^{(0)}}{\partial \tau} & = & \boldsymbol{\nabla}_y \cdot \left(\mathcal{D}_1 \boldsymbol{\nabla}_y u_{1BL}^{(0)}\right) & \text{in } Y_f^\dagger \\ \dfrac{\partial u_{2BL}^{(0)}}{\partial \tau} & = & \boldsymbol{\nabla}_y \cdot \left(\mathcal{D}_2 \boldsymbol{\nabla}_y u_{2BL}^{(0)}\right) & \\ -\mathcal{D}_1 \boldsymbol{\nabla}_y u_{1BL}^{(0)} \cdot \mathbf{n}_{fs} & = & k_1 u_{1BL}^{(0)} - k_2 u_{2BL}^{(0)} & \text{on } \partial Y_{fs}^\dagger \\ -\mathcal{D}_2 \boldsymbol{\nabla}_y u_{2BL}^{(0)} \cdot \mathbf{n}_{fs} & = & k_2 u_{2BL}^{(0)} - k_1 u_{1BL}^{(0)} & \end{array}\right. \tag{33}$$

where $u_{1BL}^{(0)}$ and $u_{2BL}^{(0)}$ are periodic in y_2 and y_3 and satisfy the boundary conditions

$$\begin{array}{lll} y_1 = 0 & c_{1D} = \sqrt{\dfrac{k_2}{k_1}} v_{0D}^{(0)} + u_{1BL(y_1=0)}^{(0)} + \psi_{1,1_{(y_1=0)}} \exp(-\lambda_1 t) v_1^{(0)}(t,\mathbf{x})_{(y_1=0)} \\ & c_{2D} = \sqrt{\dfrac{k_1}{k_2}} v_{0D}^{(0)} + u_{2BL(y_1=0)}^{(0)} + \psi_{2,1_{(y_1=0)}} \exp(-\lambda_1 t) v_1^{(0)}(t,\mathbf{x})_{(y_1=0)} \\ y_1 \to \infty & u_{1BL}^{(0)}(y_1) \to 0 \\ & u_{2BL}^{(0)}(y_1) \to 0 \\ t = 0 & u_{1BL}^{(0)} = u_{2BL}^{(0)} = 0 \end{array} \tag{34}$$

To solve the boundary problem and the upscaled model, the initial and boundary conditions for $v_0^{(0)}$, $v_1^{(0)}$, $u_{1BL}^{(0)}$ and $u_{2BL}^{(0)}$ must be specified. The boundary values of $v_0^{(0)}$, $u_{1BL}^{(0)}$ and $u_{2BL}^{(0)}$ should verify the steady state being given by (25) and (27). The boundary condition for $v_1^{(0)}$ can be legitimately adopted as $v_1^{(0)}(y_1 = 0) = 0$.

For the initial condition, owing to the compatibility condition (5) for $n = 1$, from (16) we obtain

$$\begin{array}{rcl} v_0^{(0)}(t=0,\mathbf{x}) & = & \dfrac{\sqrt{k_1 k_2}}{k_1 + k_2}\left(\langle c_1^{(0)}\rangle^f(t=0,\mathbf{x}) + \langle c_2^{(0)}\rangle^f(t=0,\mathbf{x})\right) \\ v_1^{(0)}(t=0,\mathbf{x}) & = & \dfrac{k_1\langle c_1^{(0)}\rangle^f(t=0,\mathbf{x}) - k_2\langle c_2^{(0)}\rangle^f(t=0,\mathbf{x})}{\langle \psi_{1,1}\rangle^f(k_1+k_2)} \end{array} \tag{35}$$

It is legitimate to adopt that for $\tau = 0$, no correction is needed leading to $u_{1BL}^{(0)}(\tau = 0, \mathbf{y}) = u_{2BL}^{(0)}(\tau = 0, \mathbf{y}) = 0$.

3.2.2. Order $\mathcal{O}(\varepsilon^1)$

We now construct the closure problem for the $\mathcal{O}(\varepsilon^1)$-corrective terms. First note that the steady state problem for $v_{0,\mathrm{BL}}^{(1)}$ remains unchanged. The problem for $v_{1,1\mathrm{BL}}^{(1)}$ and $v_{2,1\mathrm{BL}}^{(1)}$ to correct the terms $v_{1,1}^{(1)}$ and $v_{2,1}^{(1)}$ corresponding to the first non zero eigenvalue must be a transient problem. At short

times, inserting (32) in the initial problem (1) for c_1 and c_2, the transient problem of $v_{1,1\mathrm{BL}}^{(1)}$ and $v_{2,1\mathrm{BL}}^{(1)}$ has the same form as the problem of $v_{1,1}^{(1)}$ and $v_{2,1}^{(1)}$ given by Eq. (8) written in $\mathbf{y}$ coordinates as[6]

$$\left\{\begin{array}{rcll} \psi_{1,1}^2 \dfrac{\partial v_{1,1\mathrm{BL}}^{(1)}}{\partial \tau} & = & \boldsymbol{\nabla}_y \cdot \left(\widetilde{\mathcal{D}}_{1,1} \boldsymbol{\nabla}_y v_{1,1\mathrm{BL}}^{(1)}\right) & \text{in } Y_f^\dagger \\ \psi_{2,1}^2 \dfrac{\partial v_{2,1\mathrm{BL}}^{(1)}}{\partial \tau} & = & \boldsymbol{\nabla}_y \cdot \left(\widetilde{\mathcal{D}}_{2,1} \boldsymbol{\nabla}_y v_{2,1\mathrm{BL}}^{(1)}\right) & \\ -\widetilde{\mathcal{D}}_{1,1} \boldsymbol{\nabla}_y v_{1,1\mathrm{BL}}^{(1)} \cdot \mathbf{n}_{fs} & = & k_2\, \psi_{1,1}\, \psi_{2,1} (v_{1,1\mathrm{BL}}^{(1)} - v_{2,1\mathrm{BL}}^{(1)}) & \text{on } \partial Y_{fs}^\dagger \\ -\widetilde{\mathcal{D}}_{2,1} \boldsymbol{\nabla}_y v_{2,1\mathrm{BL}}^{(1)} \cdot \mathbf{n}_{fs} & = & k_1\, \psi_{1,1}\, \psi_{2,1} (v_{2,1\mathrm{BL}}^{(1)} - v_{1,1\mathrm{BL}}^{(1)}) & \end{array}\right. \tag{36}$$

Similar to the solution (9) for $v_{1,1}^{(1)}$ and $v_{2,1}^{(1)}$, the solution of $v_{1,1\mathrm{BL}}^{(1)}$ and $v_{2,1\mathrm{BL}}^{(1)}$ is sought in the form

$$\begin{array}{rcl} v_{1,1\mathrm{BL}}^{(1)} & = & \boldsymbol{\zeta}_1(\mathbf{y},\tau) \cdot \boldsymbol{\nabla}_x v_1^{(0)}(\mathbf{x},t) \\ v_{2,1\mathrm{BL}}^{(1)} & = & \boldsymbol{\zeta}_2(\mathbf{y},\tau) \cdot \boldsymbol{\nabla}_x v_1^{(0)}(\mathbf{x},t) \end{array} \tag{37}$$

Inserting (37) into (36), noting that the slow variable $v_1^{(0)}(\mathbf{x},t)$ is independent on the short characteristic time τ, gives rise to the local unsteady problem of the vectors $\boldsymbol{\zeta}_1$ and $\boldsymbol{\zeta}_2$

$$\left\{\begin{array}{rcll} \psi_{1,1}^2 \dfrac{\partial \boldsymbol{\zeta}_1}{\partial \tau} & = & \boldsymbol{\nabla}_y \cdot \left(\widetilde{\mathcal{D}}_{1,1} \boldsymbol{\nabla}_y \boldsymbol{\zeta}_1\right) & \text{in } Y_f^\dagger \\ \psi_{2,1}^2 \dfrac{\partial \boldsymbol{\zeta}_2}{\partial \tau} & = & \boldsymbol{\nabla}_y \cdot \left(\widetilde{\mathcal{D}}_{2,1} \boldsymbol{\nabla}_y \boldsymbol{\zeta}_2\right) & \\ -\widetilde{\mathcal{D}}_{1,1} \mathbf{n}_{fs} \cdot \boldsymbol{\nabla}_y \boldsymbol{\zeta}_1 & = & k_2\, \psi_{1,1}\, \psi_{2,1} (\boldsymbol{\zeta}_1 - \boldsymbol{\zeta}_2) & \text{on } \partial Y_{fs}^\dagger \\ -\widetilde{\mathcal{D}}_{2,1} \mathbf{n}_{fs} \cdot \boldsymbol{\nabla}_y \boldsymbol{\zeta}_2 & = & k_1\, \psi_{1,1}\, \psi_{2,1} (\boldsymbol{\zeta}_2 - \boldsymbol{\zeta}_1) & \end{array}\right. \tag{38}$$

complemented by the boundary condition at $y_1 = 0$

$$\begin{array}{rcl} \boldsymbol{\chi}_{1,1} + \boldsymbol{\zeta}_1 & = & 0 \\ \boldsymbol{\chi}_{2,1} + \boldsymbol{\zeta}_2 & = & 0 \end{array} \tag{39}$$

where $\boldsymbol{\chi}_{1,1}$ and $\boldsymbol{\chi}_{2,1}$ are solution of (10) for $n = 1$. This condition ensures that at the boundary, the terms at order $\mathcal{O}(\varepsilon)$ vanish so that only the terms at $\mathcal{O}(\varepsilon^0)$ are considered for the boundary values.

Given the solutions of the first order variables $v_0^{(0)}$ and $v_1^{(0)}$ and by solving the closure problems (29) and (38), the $\mathcal{O}(\varepsilon^1)$-correction terms $v_{0,\mathrm{BL}}^{(1)}$, $v_{1,1\mathrm{BL}}^{(1)}$ and $v_{2,1\mathrm{BL}}^{(1)}$ can be computed.

[6] Starting again from Eq. (8) with the scaling $\tau = \varepsilon^{-2} t$ on time, we would obtain (36) at order $\mathcal{O}(\varepsilon)$.

4. Numerical simulations

This section is devoted to the numerical validation of the proposed corrections to the upscaled model by considering the boundary layer either in steady state or in transient regime. For this purpose, a comparison between the numerical simulation of the corrected upscaled model and a direct numerical simulation of the Pore Scale Model (PSM) will be performed.

A porous medium of size $L \times l$ is constituted of N elementary cells of size l, composed of a solid circular inclusion of radius R located at the center of each unit cell. The radius is constrained by the porosity φ. The corresponding effective medium for the simulations of the macroscopic equations is of the same size (see Fig. 1). At the inlet $x_1 = 0$, Dirichlet conditions are applied

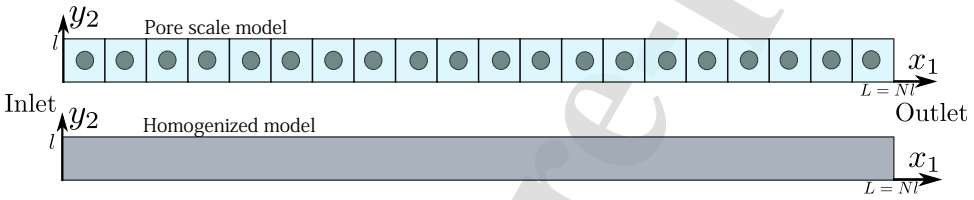

Figure 1: Porous medium and homogenized medium used in the numerical simulation.

for the concentrations $c_1 = c_{1D}$ and $c_2 = c_{2D}$. A non-equilibrium condition at the boundary $d_D = k_1 c_{1D} - k_2 c_{2D} \neq 0$ is studied. At the outlet $x_1 = L$, a zero value is imposed for the concentrations. In addition, a periodicity condition is considered for the top and bottom boundaries. The values of the physical parameters used are shown in Table 1. Note that the microscopic Damköhler numbers that constrain the values of the reaction rates k_1 and k_2 are now defined as

$$\mathrm{Da}_1 = \frac{k_1 l}{\mathcal{D}_1} \qquad \text{and} \qquad \mathrm{Da}_2 = \frac{k_2 l}{\mathcal{D}_2} = \frac{\mathrm{Da}_1 \alpha}{\beta} \tag{40}$$

with the ratios $\alpha = k_2/k_1$ and $\beta = \mathcal{D}_2/\mathcal{D}_1$.

The numerical study is carried out using COMSOL Multiphysics software based on the finite element method.

4.1. Numerical results in steady state

In steady state as $t \to \infty$, the corrections for the concentrations c_1 and c_2 are given by (19) with additional variables $u^{(0)}_{1BL}$ and $u^{(0)}_{2BL}$ (recall that as mentioned in §3.1.2 for the symmetric cell considered here the corrective term $v^{(1)}_{0,BL}$ is identically zero). First, the macroscopic variable $v^{(0)}_0$,

l	N	φ	$\mathcal{D}_1$	$\mathcal{D}_2$	β	Da_1	k_1	α	k_2	Da_2	c_{1D}	c_{2D}
0.01	20	0.8	1	$\beta\mathcal{D}_1$	2	100	$\mathrm{Da}_1\mathcal{D}_1/l$	2	αk_1	$\mathrm{Da}_1\alpha/\beta$	1	c_{1D}

Table 1: Parameters used in simulations.

solution of the homogenized diffusion problem (13) in steady state for $n = 0$ with the homogenized diffusion tensor given by (15), is computed in the effective medium. A Dirichlet boundary condition (25) is applied at the inlet whereas $v_0^{(0)} = 0$ is imposed at the outlet. If the concentrations values imposed at the interface are $c_{1D} = c_{2D} = 1$, the imposed value for $v_0^{(0)}$ corresponds to to $c_1^{(0)}(x_1 = 0) = 1.5$ and $c_2^{(0)}(x_1 = 0) = 0.75$. Secondly, given the field of $v_0^{(0)}$, the variable $v_0^{(1)}$ is determined from the solution (9) for $n = 0$

$$v_0^{(1)} = \boldsymbol{\chi} \cdot \boldsymbol{\nabla}_x v_0^{(0)} \tag{41}$$

where $\boldsymbol{\chi}$ is solution of the closure problem (11) solved numerically on the unit cell.

Finally, the correction variables $u_{1BL}^{(0)}$ and $u_{2BL}^{(0)}$, which are solutions of the local problem (20) with the boundary conditions at the inlet given by (27) and a zero-value condition far from the inlet, are solved in the microscopic pore-geometry for at least several unit cells from the inlet due to the exponential-decay behavior of these functions. This point will be proved in the numerical results in the sequel.

Let define the y_2-average operator of a function f as

$$\langle f \rangle_{y_2} = \frac{1}{l} \int_0^l f dy_2 \tag{42}$$

Figure 2(a) displays the variation of the y_2-averaged variables $\langle u_{1BL}^0 \rangle_{y_2}$ and $\langle u_{2BL}^0 \rangle_{y_2}$ with respect to the position x_1/L. We can observe that the correction u_{1BL}^0 (respectively u_{2BL}^0) decreases (respectively increases) rapidly and decays towards zero after several unit cells in the vicinity of the inlet. Thus, this correction only affects a thin layer (boundary layer) from the edge whose thickness depends on the Damköhler numbers. The variation of the difference $\langle d_{BL}^0 \rangle_{y_2}$ with respect to x_1/L is plotted in Figure 2(b). It is clearly observed that a non-equilibrium state where $\langle d_{BL}^0 \rangle_{y_2} \neq 0$ is established in a thin boundary layer.

Given the solutions for $v_0^{(0)}$, $v_0^{(1)}$, $u_{1BL}^{(0)}$ and $u_{2BL}^{(0)}$, knowing that $v_{0,BL}^{(1)} \equiv 0$, the y_2-averaged concentrations $\langle c_i \rangle_{y_2}$ of the corrected model can be computed from (19). In order to compare these results with the solution of the original model, the non-corrected homogenized model (HM)

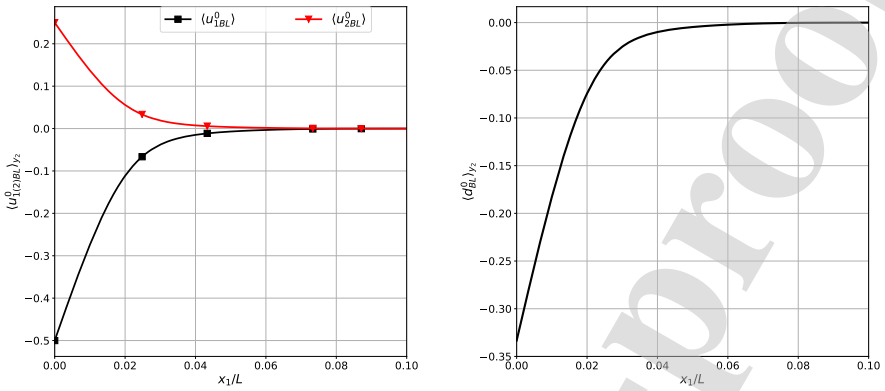

(a) (b)

Figure 2: Variation of (a): $\langle u^0_{1BL}\rangle_{y_2}$ and $\langle u^0_{2BL}\rangle_{y_2}$ and (b): $\langle d^0_{BL}\rangle_{y_2}$ versus x_1/L for $\mathrm{Da}_1 = 100$.

given by the system (17) is solved in the effective porous media. To do that, we first compute the eigenvalue λ_1 and the eigenfunctions $\psi_{1,1}$ and $\psi_{2,1}$ from the spectral problem (2) for $n = 1$. Given the eigenfunctions, the closure problem (10) for $\boldsymbol{\chi}_{1,1}$ and $\boldsymbol{\chi}_{2,1}$ is solved in the unit cell to compute the effective coefficient $\mathbf{D}_{v,1}$ from (14) for $n = 1$. Moreover, the closure problem for $\boldsymbol{\chi}$ in (11) is purely geometric and is solved in the unit cell to give the effective tensor $\mathbf{D}_{v,0}$ from (15).

To validate the proposed corrections in steady state, a direct numerical simulation of the pore-scale model (PSM) given in Eq. (1) is performed with the pore-scale geometry of Figure 1 to obtain the concentration fields which are averaged over the y_2 direction. Figure 3 displays the y_2-averaged concentration profiles of $\langle c_1\rangle_{y_2}$ and $\langle c_2\rangle_{y_2}$ obtained from the corrected model (continuous line), the original HM without correction (dotted line) and the PSM (line-marker). An excellent agreement between the corrected model and the PSM is observed, which satisfactorily validates the proposed model. The original HM solution fails to capture the complex physics in the boundary layer and leads to an inaccurate prediction of the concentration fields in the entire domain. We can also observe that $\langle c_1\rangle_{y_2}$ (respectively $\langle c_2\rangle_{y_2}$) increases (respectively decreases) quickly in the boundary layer to attain a transition point delimiting the boundary zone.

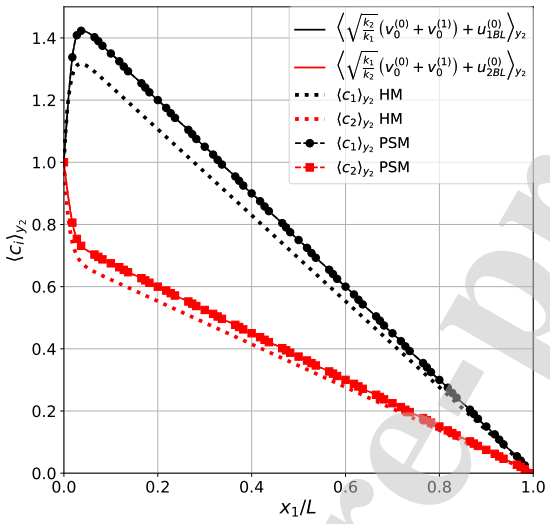

Figure 3: y_2-averaged concentrations versus x_1/L for $\mathrm{Da}_1 = 100$ obtained by the corrected model (line), the original HM (dotted line) and the PSM (line-marker).

4.2. Numerical results in transient regime

The corrected solution for the concentrations involving additional variables at order $\mathcal{O}(\varepsilon^1)$ in transient regime is given by Eq. (32). To compute the concentrations, first we solve the transient problems for the first-order variables $v_0^{(0)}$ and $v_1^{(0)}$ given by (13) with the initial conditions (35). In addition, the Dirichlet boundary condition for $v_0^{(0)}$ (25) is imposed at the inlet and $v_0^{(0)} = 0$ at the outlet whereas for $v_1^{(0)}$, the zero value is imposed on both boundaries. Given the fields of $v_0^{(0)}$ and $v_1^{(0)}$, the $\mathcal{O}(\varepsilon^1)$-variables $v_0^{(1)}$, $v_{1,1}^{(1)}$ and $v_{2,1}^{(1)}$ can be computed from the solution (9).

The first-order corrections $u_{1,BL}^{(0)}$ and $u_{2,BL}^{(0)}$ for the unsteady state in (33) can be solved on several unit cells adjacent to the boundary with a boundary condition similar to that given in the steady state and with a zero initial value. To compute the $\mathcal{O}(\varepsilon^1)$-correction variables, as $v_{0,\mathrm{BL}}^{(1)} \equiv 0$ accounting for the symmetry of the elementary cell considered (see section 3.1.2), for determining $v_{1,1\mathrm{BL}}^{(1)}$ and $v_{2,1\mathrm{BL}}^{(1)}$ given by (37), one has to solve the unsteady closure problem (38) for $\boldsymbol{\zeta}_1$ and $\boldsymbol{\zeta}_2$ with the corresponding boundary condition (39).

In order to validate the proposed corrected model, a direct numerical simulation of the PSM (Eq. 1) is numerically solved in the pore-scale geometry in transient regime. Initial values of the concentrations are imposed as $c_1(t=0) = c_2(t=0) = 0.1$, which corresponds to a non-equilibrium initial state. Parameters used in the simulation are given in Table 1. Moreover, macroscopic equations without correction (17) are also numerically solved in the same geometry.

Figure 4 shows the variation of the y_2-averaged concentrations $\langle c_1 \rangle_{y_2}$ and $\langle c_2 \rangle_{y_2}$ with time at different positions $x_1 = [l/4, 2l, 3l]$, obtained from the corrected model, the original homogenized model (HM) and the direct numerical simulation of the pore-scale model (PSM). Excellent agreement is obtained between the PSM and the corrected model for the three observation points located at different x_1 positions, which satisfactorily validates the proposed transient model. At very short times when the local chemical reaction dominates the transport mechanism and the boundary layer is located very close to the surface, all three models predict the same results at the observation points. However, for longer times, when the boundary layer propagates through the domain, a difference between the original HM and the PSM appears and this is all the earlier as the position of the point is close to the surface at the left boundary.

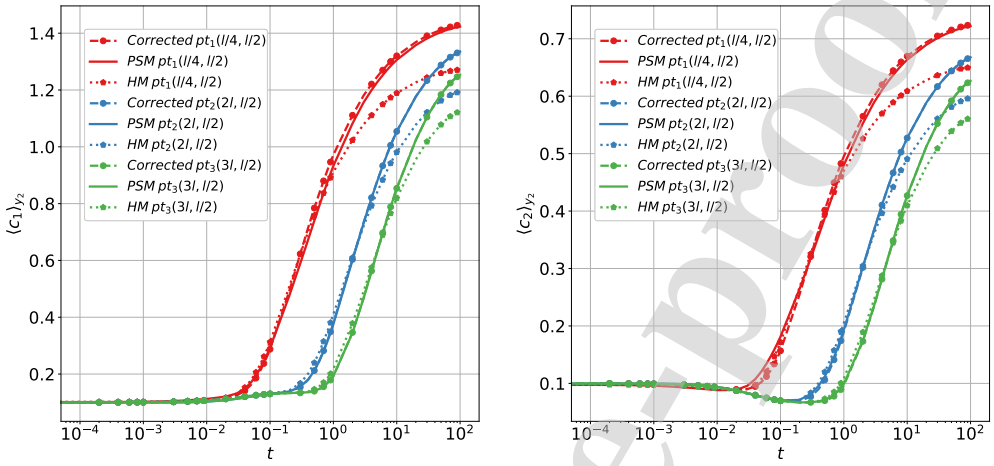

(a) $\langle c_1 \rangle_{y_2}$ versus time.

(b) $\langle c_2 \rangle_{y_2}$ versus time.

Figure 4: Concentration variation of (a) $\langle c_1 \rangle_{y_2}$ and (b) $\langle c_2 \rangle_{y_2}$ with time for different positions $x_1 = [l/4, 2l, 3l]$, obtained from the corrected model (dashed line-marker), PSM (line) and the original HM (dotted line-marker).

Figures 5 and 6 display the y_2-averaged concentration profiles of $\langle c_1 \rangle_{y_2}$ and $\langle c_2 \rangle_{y_2}$ with respect to x_1/L obtained from the three models at different times t. Small fluctuations in the concentrations obtained by the corrected model are observed at the beginning of the process due to the periodic variation of the eigenfunctions, which vanish with time. Again, the corrected model is in very good agreement with the PSM while the original HM fails to reproduce the boundary layer behavior correctly. As a result, this error propagates with time away from the boundary, leading to inaccurate prediction of concentration profiles.

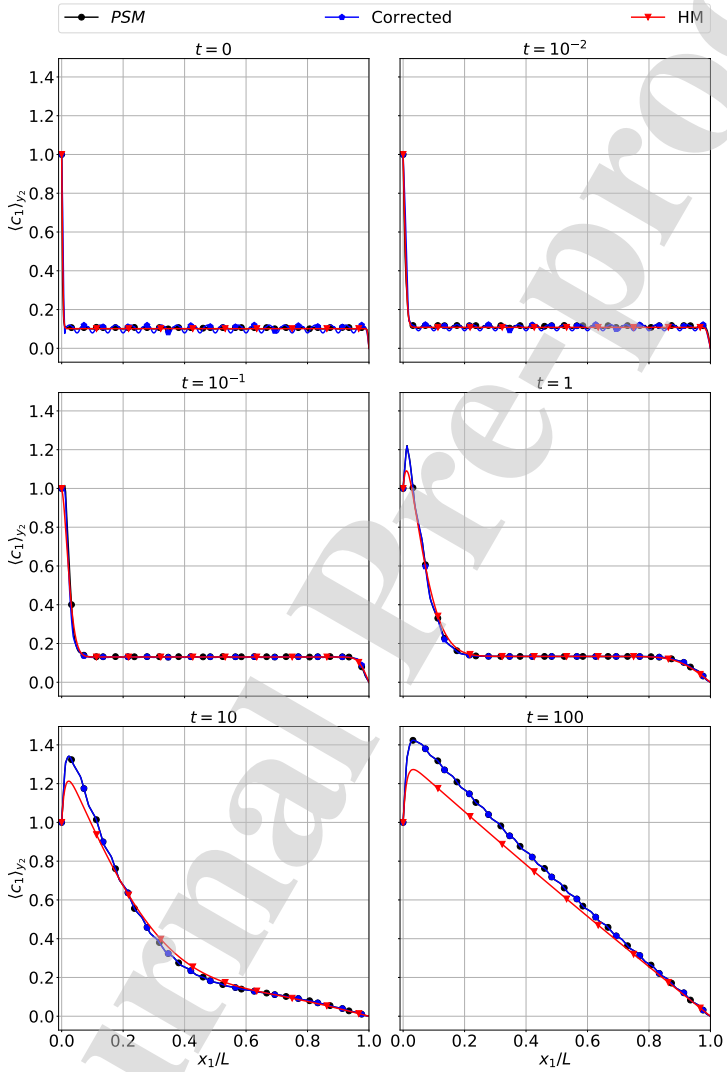

Figure 5: Concentration $\langle c_1 \rangle_{y_2}$ versus x_1/L for different times.

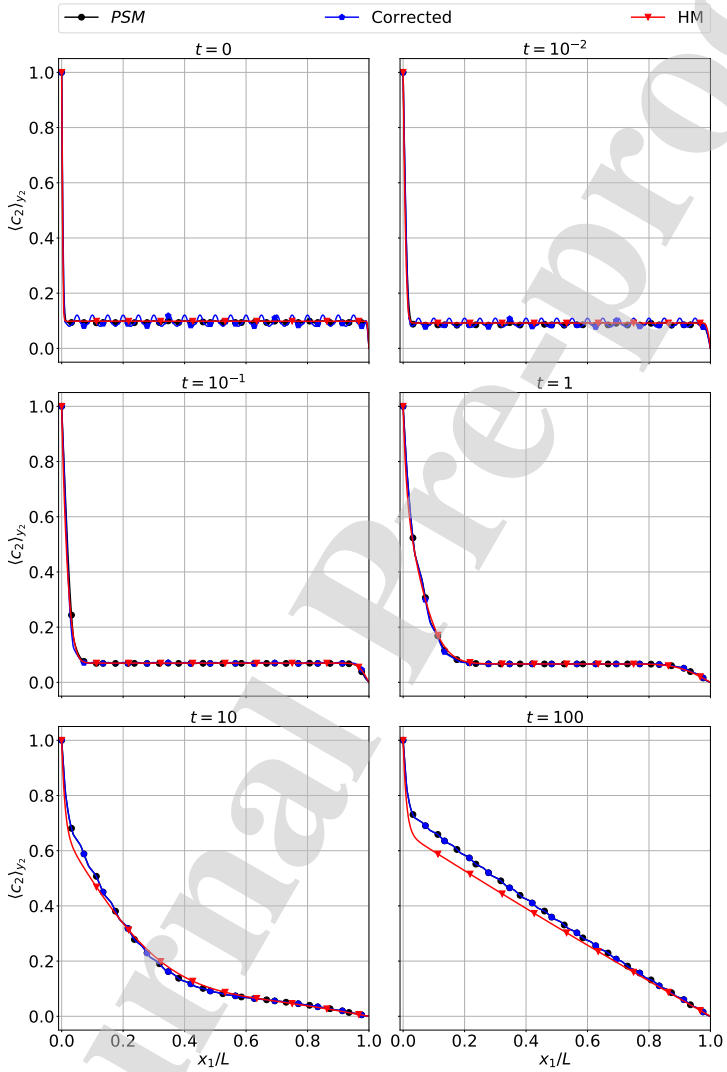

Figure 6: Concentration $\langle c_2 \rangle_{y_2}$ versus x_1/L for different times.

Finally to quantify the role of each term in the solution (32), Figure 7a shows the profiles of the terms corresponding to $n = 0$ at very short times. The correction $u^{(0)}_{1,BL}$ tends towards zero rapidly from the boundary as shown previously and dominates the correction $v^{(1)}_{0,BL}$, which is of order $\mathcal{O}(\varepsilon)$ in the general case and vanishes for symmetric elementary cells, which is the case here. Far from the boundary, only the first-order variable $v^{(0)}_0$ differs significantly from zero. In Figure 7b, the terms corresponding to $n = 1$ are plotted. The fluctuations are due to the periodic solution of the eigenfunction $\psi_{1,1}$. Due to exponential decay, the terms disappear over time. We observe that the time-dependent correction terms at this order are very small and can be neglected.

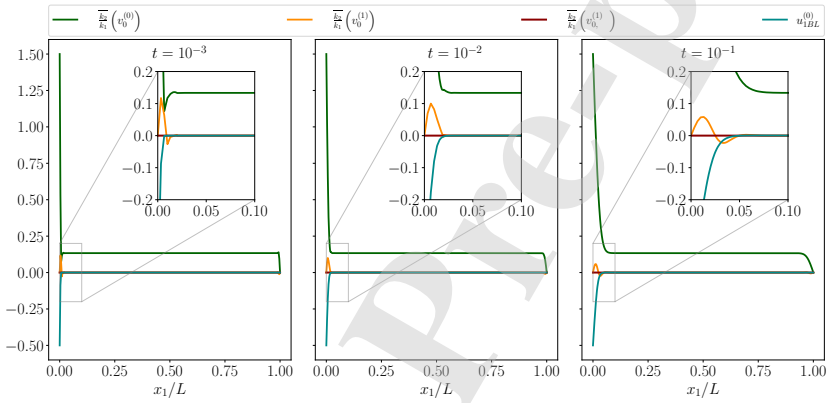

(a)

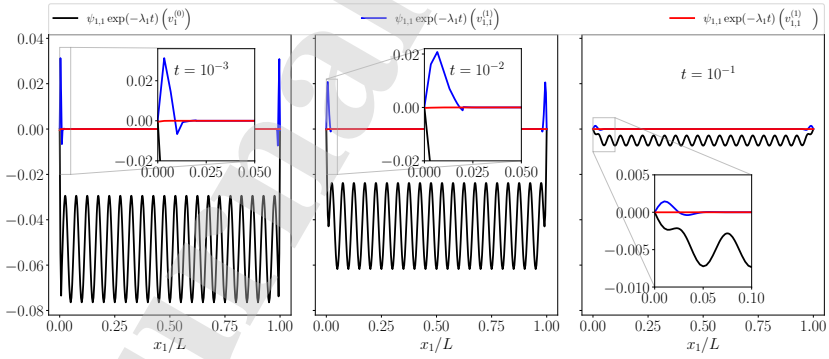

(b)

Figure 7: Corrective term profiles for different times.

5. Conclusion

The boundary layer problem for the coupled diffusion/reaction process for high Damköhler number in porous media has been studied. The macroscopic mass conservation law derived from the homogenization technique and based on a spectral approach represents a quasi-exact solution within the domain but fails to describe the physics in a thin layer near the surface when a non-equilibrium Dirichlet boundary condition is imposed. In this context, corrective terms have to be added to the concentrations for both steady state and transient regime.

In steady state, two corrective functions are introduced to adjust the first order variable corresponding to the null eigenvalue to capture the non-equilibrium state in the boundary layer. These terms decay exponentially from the boundary and need to be solved only on a few unit cells adjacent to the boundary. Numerical simulations prove that this correction is in excellent agreement with the direct numerical simulation of the pore-scale model.

In transient regime, the $\mathcal{O}(\varepsilon)$-variables need to be corrected with additional terms whose solutions involve new closure problems. Numerical results show a small contribution of these terms.

References

[1] G. Allaire, R. Brizzi, A. Mikelic, A. Piatnitski, Two-scale expansion with drift approach to the Taylor dispersion for reactive transport through porous media, Chemical Engineering Science 65 (7) (2010) 2292–2300.

[2] J.-F. Bloch, J.-L. Auriault, Upscaling of diffusion-reaction phenomena by homogenisation technique: Possible appearance of morphogenesis, Transport in Porous Media 127 (1) (2019) 191–209.

[3] I. Battiato, D. M. Tartakovsky, Applicability regimes for macroscopic models of reactive transport in porous media, Journal of Contaminant Hydrology 120-121 (Supplement C) (2011) 18–26.

[4] F. Boso, I. Battiato, Homogenizability conditions for multicomponent reactive transport, Advances in Water Resources 62 (Part B) (2013) 254–265.

[5] H. D. Lugo-Méndez, F. J. Valdés-Parada, M. L. Porter, B. D. Wood, J. A. Ochoa-Tapia, Upscaling diffusion and nonlinear reactive mass transport in homogeneous porous media, Transport in Porous Media 107 (3) (2015) 683–716.

[6] A. Tartakovsky, D. Tartakovsky, T. Scheibe, P. Meakin, Hybrid simulations of reaction-diffusion systems in porous media, SIAM Journal on Scientific Computing 30 (6) (2008) 2799–2816.

[7] T. Qiu, Q. Wang, C. Yang, Upscaling multicomponent transport in porous media with a linear reversible heterogeneous reaction, Chemical Engineering Science 171 (2017) 100–116.

[8] F. J. Valdés-Parada, C. G. Aguilar-Madera, J. Alvarez-Ramirez, On diffusion, dispersion and reaction in porous media, Chemical Engineering Science 66 (10) (2011) 2177–2190.

[9] F. J. Valdés-Parada, D. Lasseux, S. Whitaker, Diffusion and heterogeneous reaction in porous media: The macroscale model revisited, International Journal of Chemical Reactor Engineering 15 (6) (2017) 1–24.

[10] G. Allaire, A.-L. Raphael, Homogenization of a convection–diffusion model with reaction in a porous medium, Comptes Rendus Mathematique 344 (8) (2007) 523–528.

[11] M. K. Bourbatache, O. Millet, C. Moyne, Upscaling diffusion–reaction in porous media, Acta Mechanica 231, 2011–2031 (2020) 2011–2031. doi:10.1007/s00707-020-02631-9.

[12] R. Mauri, Dispersion, convection, and reaction in porous media, Physics of Fluids A: Fluid Dynamics 3 (5) (1991) 743–756.

[13] M. K. Bourbatache, O. Millet, C. Moyne, Upscaling coupled heterogeneous diffusion reaction equations in porous media., Accepted in Acta Mechanica (2023).

[14] T. D. Le, C. Moyne, M. K. Bourbatache, O. Millet, A spectral approach for homogenization of diffusion and heterogeneous reaction in porous media, Applied Mathematical Modelling 104 (2022) 666–681.

[15] M. K. Bourbatache, O. Millet, T. D. Le, C. Moyne, Homogenized model for diffusion and heterogeneous reaction in porous media: numerical study and validation, Applied Mathematical Modelling 111 (2022) 486–500.

[16] H. Dumontet, Study of a boundary layer problem in elastic composite materials, Mathematical Modelling and Numerical Analysis 20 (1986) 265–286.

[17] S. Koley, C. Upadhyay, P. Mohite, Study of boundary layer effects at ply interfaces of laminated composites using homogenization theory, Composite Structures 286 (2022) 1–21.

[18] N. Buannic, P. Cartraud, Higher-order effective modelling of periodic heterogeneous beams. II. Derivation of the proper boundary conditions for the interior asymptotic solution, International Journal of Solids and Structures 38 (2001) 7163–7180.

[19] P. Destuynder, Sur une justification des modèles de plaques et de coques par les méthodes asymptotiques, Thèse d'état, Paris (1979).

[20] G. Allaire, M. Amar, Boundary layer tails in periodic homogenization, ESAIM: Control, Optimisation and Calculus of Variations 4 (1999) 209–243.

[21] M. Amar, M. Tarallo, S. Terracini, On the exponential decay for boundary layer, C. R. Acad. Sci, Paris, Série I 328 (1999) 1139–1144.

[22] A. Matine, N. Boyard, P. Cartraud, G. Legrain, Y. Jarny, Modeling of thermophysical properties in heterogeneous periodic media according to a multi-scale approach: Effective conductivity tensor and edge effects, International Journal of Heat and Mass Transfer 62 (2013) 586–603.

[23] A. Matine, N. Boyard, G. Legrain, Y. Jarny, P. Cartraud, Transient heat conduction within periodic heterogeneous media: A space-time homogenization approach, International Journal of Thermal Sciences 92 (2015) 217–229.

[24] K. Bourbatache, T. D. Le, O. Millet, C. Moyne, Limits of classical homogenization procedure for coupled diffusion-heterogeneous reaction processes in porous media, Transport in Porous Media 140 (2021) 437–457.

[25] R. B. Bird, W. E. Stewart, E. N. Lightfoot, Transport Phenomena, John Wiley & Sons (2007).

- Boundary layer problem of diffusion/reaction process in porous media is studied
- Macro-model derived from homogenization technique and spectral approach is recalled
- Corrective terms are introduced to modify the concentration's expansion
- These terms decay rapidly from the boundary and are solved on several unit cells
- Numerical simulations highlight the role of the corrective terms in boundary layer

Tien Dung Le: Conceptualization; Methodology; Roles/Writing - original draft; Writing - review & editing, **Christian Moyne**: Conceptualization; Methodology; Roles/Writing - original draft, **Khaled Bourbatache**: Conceptualization; Methodology; Software; Roles/Writing - original draft; Writing - review & editing, **Olivier Millet**: Conceptualization; Methodology; Roles/Writing - original draft; Writing - review & editing

Declaration of interests

☒ The authors declare that they have no known competing financial interests or personal relationships that could have appeared to influence the work reported in this paper.

☐ The authors declare the following financial interests/personal relationships which may be considered as potential competing interests: